

See discussions, stats, and author profiles for this publication at: <https://www.researchgate.net/publication/12178827>

Syntheses and Relaxation Properties of Mixed Gadolinium Hydroxypyridinonate MRI Contrast Agents

ARTICLE *in* INORGANIC CHEMISTRY · DECEMBER 2000

Impact Factor: 4.76 · DOI: 10.1021/ic000563b · Source: PubMed

CITATIONS

85

READS

21

7 AUTHORS, INCLUDING:



Mauro Botta

Amedeo Avogadro University of Eastern Pied...

252 PUBLICATIONS 8,429 CITATIONS

SEE PROFILE



Alessandro Barge

Università degli Studi di Torino

98 PUBLICATIONS 2,398 CITATIONS

SEE PROFILE



Silvio Aime

Università degli Studi di Torino

671 PUBLICATIONS 17,700 CITATIONS

SEE PROFILE

Syntheses and Relaxation Properties of Mixed Gadolinium Hydroxypyridinonate MRI Contrast Agents

Seth M. Cohen, Jide Xu, Emil Radkov, and Kenneth N. Raymond*

Department of Chemistry, University of California, Berkeley, California 94720

Mauro Botta

Dipartimento di Scienze e Tecnologie Avanzate, Università del Piemonte Orientale
“Amedeo Avogadro”, Corso Borsalino 54, 15100 Alessandria, Italy

Alessandro Barge and Silvio Aime*

Dipartimento di Chimica IFM, Università di Torino, Via P. Giuria 7, 10125 Torino, Italy

Received May 24, 2000

The tripodal ligand tris[(3-hydroxy-1-methyl-2-oxo-1,2-didehydropyridine-4-carboxamido)ethyl]amine (TREN-Me-3,2-HOPO) forms a stable Gd^{3+} complex that is a promising candidate as a magnetic resonance imaging (MRI) contrast agent. However, its low water solubility prevents detailed magnetic characterization and practical applicability. Presented here are a series of novel mixed ligand systems that are based on the TREN-Me-3,2-HOPO platform. These new ligands possess two hydroxypyridinone (HOPO) chelators and one other chelator, the latter of which can be easily functionalized. The ligands described use salicylamide, 2-hydroxyisophthalamide, 2,3-dihydroxyterephthalamide, and bis(acetate) as the derivatizable chelators. The solution thermodynamics and relaxivity properties of these new systems are presented. Three of the four complexes (salicylamide-, 2-hydroxyisophthalamide-, and 2,3-dihydroxyterephthalamide-based ligands) possess sufficient thermodynamic stability for in vivo applications. The relaxivities of the three corresponding Gd^{3+} complexes range from 7.2 to 8.8 $\text{mM}^{-1} \text{s}^{-1}$ at 20 MHz, 25 °C, and pH 8.5, significantly higher than the values for the clinically employed polyaminocarboxylate complexes (3.5–4.8 $\text{mM}^{-1} \text{s}^{-1}$). The high relaxivities of these complexes are consistent with their faster rates of water exchange (<100 ns), higher molecular weights (>700), and greater numbers of inner-sphere coordinated water molecules ($q = 2$) relative to those of polyaminocarboxylate complexes. A mechanism for the rapid rates of water exchange is proposed involving a low energy barrier between the 8- and 9-coordinate geometries for lanthanide complexes of HOPO-based ligands. The pathway is supported by the crystal structure of $\text{La}[\text{TREN-Me-3,2-HOPO}]$ (triclinic $P\bar{1}$: $Z = 4$, $a = 15.6963(2) \text{ \AA}$, $b = 16.9978(1) \text{ \AA}$, $c = 17.1578(2) \text{ \AA}$, $\alpha = 61.981(1)^\circ$, $\beta = 75.680(1)^\circ$, $\gamma = 71.600(1)^\circ$), which shows both 8- and 9-coordinate metal centers in the asymmetric unit, demonstrating that these structures are very close in energy. These properties make heteropodate Gd^{3+} complexes promising candidates for use in macromolecular contrast media, particularly at higher magnetic field strengths.

Introduction

Complexes of gadolinium are important for their use as commercial magnetic resonance imaging (MRI) contrast agents. The novel complex $\text{Gd}[\text{TREN-Me-3,2-HOPO}]$ has been shown to possess several advantageous features for use as an MRI contrast agent,^{1–4} including low toxicity, high stability (pGd 20.3), and high relaxivity (10 $\text{mM}^{-1} \text{s}^{-1}$).⁵ To further exploit the excellent properties of $\text{Gd}[\text{TREN-Me-3,2-HOPO}]$, a number

of attempts have been made to functionalize the ligand in order to improve the water solubility of the Gd^{3+} complex. Initial studies focused on modifying the hydroxypyridinone (HOPO) ring system⁶ and synthesizing substituted tris(2-aminoethyl)-amine (TREN) scaffolds.^{7,8} An alternative ligand design is to prepare mixed ligand systems that are more directly amenable to substitution. Described here are tripodal ligands formed from two HOPO chelators and a third binding group that can be easily functionalized. The third chelating moiety of these “heteropodands” can tune various properties of the ligand and the resulting metal complex, including denticity, charge, solubility, and stability.

* To whom correspondence should be addressed.

- (1) Aime, S.; Botta, M.; Fasano, M.; Terreno, E. *Acc. Chem. Res.* **1999**, *32*, 941.
- (2) Caravan, P.; Ellison, J. J.; McMurry, T. J.; Lauffer, R. B. *Chem. Rev.* **1999**, *99*, 2293.
- (3) Aime, S.; Botta, M.; Fasano, M.; Terreno, E. *Chem. Soc. Rev.* **1998**, *27*, 19.
- (4) Tweedle, M. F. In *Relaxation Agents in NMR Imaging*; Bunzli, J.-C. G., Choppin, G. R., Eds.; Elsevier: Amsterdam, 1989; p 127.
- (5) Xu, J.; Franklin, S. J.; Whisenhunt, D. W., Jr.; Raymond, K. N. *J. Am. Chem. Soc.* **1995**, *117*, 7245.

- (6) Johnson, A.; O'Sullivan, B.; Raymond, K. N. *Inorg. Chem.* **2000**, *39*, 2652.
- (7) Hajela, S.; Botta, M.; Giraudo, S.; Xu, J.; Raymond, K. N.; Aime, S., in press.
- (8) Hajela, S.; Johnson, A.; Sunderland, C. J.; Xu, J.; Cohen, S. M.; Caulder, D. L.; Raymond, K. N. Manuscript in preparation.

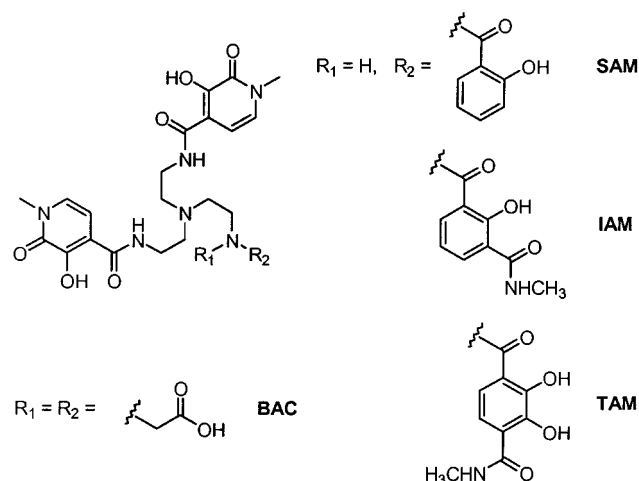


Figure 1. Diagram of the ligands examined in this study. The ligands are designated TREN-Me-3,2-HOPO- followed by the suffixes indicated in the figure.

This work details the syntheses of heteropodands that possess sites for facile functionalization (Figure 1). These ligands use an (Me-3,2-HOPO)-substituted TREN compound as an universal intermediate. The syntheses, solution thermodynamics, and relaxivity properties of these systems are described. The results indicate that three of the ligand systems described have properties desirable for new MRI imaging agents, including high relaxivity and thermodynamic stability. Among the most notable attributes is an extremely rapid water exchange rate (30–100 ns) that makes these complexes amenable to incorporation into macromolecular structures. The rapid water exchange rate is due to a low-energy barrier between the 8- and 9-coordinate metal complexes. This hypothesis is supported by the crystal structure of La[TREN-Me-3,2-HOPO], which shows both coordination numbers at the metal ion in the same unit cell. The findings suggest that an HOPO-based heteropodand ligand strategy has substantial promise for designing MRI contrast agents.

Experimental Section

Syntheses. General Information. Unless otherwise noted, starting materials were obtained from commercial suppliers and used without further purification. Tris(2-aminoethyl)amine was distilled under vacuum from CaH₂. Flash silica gel chromatography was performed using Merck 40–70 mesh silica gel. Microanalyses were performed at the Microanalytical Services Laboratory, College of Chemistry, University of California, Berkeley. Mass spectra were recorded at the Mass Spectrometry Laboratory, College of Chemistry, University of California, Berkeley. All NMR spectra were recorded either on an AMX 300 or 400 Bruker superconducting Fourier transform spectrometer or on a DRX 500 Bruker superconducting digital spectrometer. Infrared spectra were obtained using a Nicolet Magna IR 550 Fourier transform spectrometer. The syntheses of the terephthalamide heteropodand, TREN-Me-3,2-HOPOTAM, and the isophthalamide heteropodand, TREN-Me-3,2-HOPOIAM, are described elsewhere.⁹

Protected TREN-Me-3,2-HOPOSAM (1). (3,2-HOPO)₂TREN⁹ (2.2 mmol) was dissolved in 70 mL of dry CH₂Cl₂. This solution was added to a solution of 2-(benzyloxybenzoyl)succinimide (2.6 mmol) dissolved in 30 mL of dry CH₂Cl₂. After 2 h, the resulting solution was evaporated to dryness, affording an amber oil. The oil was purified by silica column chromatography with 0–8% MeOH in CH₂Cl₂ as the eluant. Removal of solvent gave the product as a white foam. Yield: 78%. IR (film from CH₂Cl₂): ν 1538, 1645, 3384 cm⁻¹. ¹H NMR (300 MHz, CDCl₃, 25 °C): δ 2.25 (t, *J* = 6.7 Hz, 4H, CH₂), 2.36 (t, *J* = 6.5 Hz, 2H,

CH₂), 3.08 (q, *J* = 6.0 Hz, 4H, CH₂), 3.24 (q, *J* = 5.8 Hz, 2H, CH₂), 3.57 (s, 6H, NCH₃), 5.04 (s, 2H, CH₂), 5.27 (s, 4H, CH₂), 6.66 (d, *J* = 7.2 Hz, 2H, Ar H), 6.96 (d, *J* = 8.2 Hz, 1H, Ar H), 7.05 (d, *J* = 7.2 Hz, 2H, Ar H), 7.30 (m, 17H, Ar H), 7.76 (t, *J* = 5.2 Hz, 2H, NH), 7.85 (br t, 1H, NH), 8.11 (d, *J* = 6.0 Hz, 1H, Ar H). ¹³C NMR (400 MHz, CDCl₃, 25 °C): δ 34.0, 37.2, 37.6, 37.7, 52.0, 52.2, 71.2, 74.7, 104.7, 112.7, 121.4, 121.9, 127.8, 128.6, 128.7, 128.8, 129.0, 130.8, 132.1, 132.2, 132.4, 135.8, 136.3, 146.2, 156.6, 159.5, 163.3, 165.2. Anal. Calcd (found) for C₄₈H₅₀N₆O₈·2H₂O: C, 65.89 (66.13); H, 6.22 (5.93); N, 9.60 (9.97). (+)-FABMS: *m/z* 839 [M⁺ + H].

TREN-Me-3,2-HOPOSAM (2). **1** (1.8 mmol) was dissolved in 40 mL of 1:1 concentrated HCl/glacial acetic acid. After 18 h of stirring, the solution was evaporated to dryness. The residue was coevaporated with 4 × 20 mL of MeOH and then oven-dried, giving a pale yellow solid. Yield: 79%. IR (KBr pellet): ν 1540, 1594, 3255 cm⁻¹. ¹H NMR (300 MHz, CD₃OD, 25 °C): δ 3.35 (s, 6H, NCH₃), 3.59 (br s, 6H, CH₂), 3.76 (br s, 6H, CH₂), 6.18 (br s, 2H, Ar H), 6.62 (br s, 2H, Ar H), 6.71 (d, *J* = 7.2 Hz, 2H, Ar H), 7.17 (br t, 1H, Ar H), 7.47 (br d, 1H, Ar H). ¹³C NMR (400 MHz, DMSO-*d*₆, 25 °C): δ 34.4, 37.1, 52.1, 75.3, 103.0, 115.5, 116.6, 117.5, 119.0, 127.9, 128.5, 134.1, 148.0, 158.3, 159.8, 166.9, 169.8. Anal. Calcd (found) for C₂₇H₃₃N₆O₈Cl·MeOH·0.5HCl: C, 51.32 (51.24); H, 5.77 (5.58); N, 12.82 (12.55). (+)-FABMS: *m/z* 569 [M⁺ + H].

TREN-Me-3,2-HOPOBAC (3). (3,2-HOPO)₂TREN⁹ (3.2 mmol), benzyl 2-bromoacetate (10 mmol), and anhydrous K₂CO₃ (10 mmol) were combined in dry THF (50 mL). The stirred mixture was warmed to 60 °C overnight under N₂(g). After the system had cooled to room temperature, the reaction mixture was filtered, the filtrate was rotary-evaporated, and the residue was applied to a flash silica gel column. Elution with 0.5–4.0% CH₃OH in CH₂Cl₂ produced a pale yellow, thick oil as the pure benzyl-protected precursor. The ligand was immediately deprotected by dissolving the protected precursor in glacial acetic acid (20 mL) containing 20% Pd(OH)₂ on charcoal catalyst (200 mg). The mixture was stirred under an atmosphere of H₂(g) (400 psi) at room temperature overnight. The solution was filtered, and the filtrate was evaporated to dryness, affording a pale brown residue. The residue was recrystallized from methanol to give **3** as a white powder. Yield: 53%. ¹H NMR (500 MHz, D₂O, 25 °C): δ 3.29 (br s, 4H, CH₂), 3.37 (s, 6H, CH₂), 3.40–3.42 (br m, 2H, CH₂), 3.54 (br s, 4H, CH₂), 3.79 (s, 6H, NCH₃), 6.351 (d, *J* = 4.3 Hz, 2H, Ar H), 6.839 (d, *J* = 4.3 Hz, 2H, Ar H). ¹³C NMR (500 MHz, DMSO-*d*₆, 25 °C): ν 36.33, 36.85, 51.08, 51.68, 55.77, 102.55, 116.67, 127.43, 148.12, 158.05, 165.83, 172.26. (+)-FABMS: *m/z* 565 [M⁺ + H]. Anal. Calcd (found) for C₂₄H₃₂N₆O₁₀·1.2H₂O: C, 49.17 (49.68); H, 5.91 (6.15); N, 14.33 (13.98).

HGd[TREN-Me-3,2-HOPOTAM]. TREN-Me-3,2-HOPOTAM (0.10 mmol) was dissolved in 10 mL of MeOH. Gd(NO₃)₃·6H₂O (0.10 mmol) was added to the methanol solution, followed by an excess of pyridine, which caused the precipitation of an off-white solid. The mixture was heated to reflux for 2 h and was then evaporated to dryness. The residue was then suspended in ³PrOH. This was followed by sonication, and filtration to give the acid complex final product. (–)-FABMS: *m/z* 795 [M[–]].

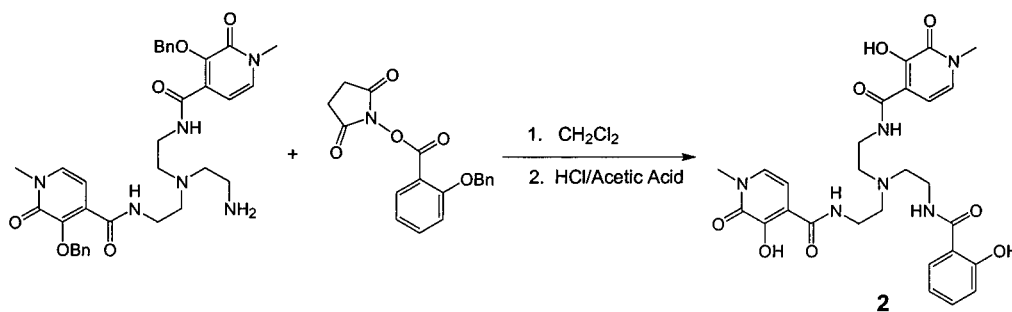
Gd[TREN-Me-3,2-HOPOIAM]. TREN-Me-3,2-HOPOIAM (0.10 mmol) was dissolved in 10 mL of MeOH. Gd(NO₃)₃·6H₂O (0.10 mmol) was added to the methanol solution, followed by an excess of pyridine. The mixture was heated to reflux for 2 h and was then evaporated to dryness. The residue was suspended in ³PrOH, followed by sonication and filtration. (+)-FABMS: *m/z* 781 [M⁺ + H].

Gd[TREN-Me-3,2-HOPOSAM]. **2** (0.20 mmol) was dissolved in 10 mL of MeOH. Gd(NO₃)₃·6H₂O (0.20 mmol) was added to the methanol solution, followed by an excess of pyridine, which caused the precipitation of an off-white solid. The mixture was refluxed for 2 h and was then evaporated to dryness. The residue was suspended in ³PrOH, followed by sonication and filtration. (+)-FABMS: *m/z* 724 [M⁺ + H].

KGd[TREN-Me-3,2-HOPOBAC]. To a solution of **3** (0.20 mmol) in dry methanol (20 mL) was added 4 equiv of KOH solution in methanol (0.1027 N) to neutralize the ligand. A solution of GdCl₃·6H₂O (0.18 mmol) in methanol (10 mL) was added slowly to the ligand solution with stirring. The mixture was heated to reflux for 6 h under

(9) Cohen, S. M.; O'Sullivan, B.; Raymond, K. N. *Inorg. Chem.*, in press.

Scheme 1



nitrogen. The solvent was then removed, and the residue was purified twice on a Sephadex column eluted with methanol. The complex was precipitated from a 3:1 mixture of THF/MeOH, washed with THF, and vacuum-dried. (–)-FABMS: m/z 717 [M[–]].

Structure Determination and Refinement of La[TREN-Me-3,2-HOPO]. The X-ray data collection and structure solution and refinement procedures were as previously described.^{10–12} Crystals were grown as colorless rhomboids from a solution of the complex in DMSO diffused with MeOH (Table 3). The complex crystallized in the space group $P\bar{1}$ (No. 2), with $a = 15.6963(2)$ Å, $b = 16.9978(1)$ Å, $c = 17.1578(2)$ Å, $\alpha = 61.981(1)^\circ$, $\beta = 75.680(1)^\circ$, $\gamma = 71.600(1)^\circ$, and $Z = 4$. Data were corrected for Lorentz and polarization effects, and an empirical absorption was applied using XPREP (ellipsoidal model; $T_{\max} = 0.931$ and $T_{\min} = 0.702$). Two different metal centers were found in the asymmetric unit (see Results and Discussion and Figure 9). All of the solvent molecules found, one DMSO (0.2 occupancy) and five MeOH (varying occupancy of 0.25 to full) molecules, were severely disordered. All non-hydrogen atoms except those of the disordered groups and solvent were refined anisotropically. Hydrogen atoms were assigned to idealized positions. Final refinement for 8738 observations, 917 parameters, and 52 restraints gave $R1 = 0.0710$, $wR2 = 0.1659$, and $GOF = 1.038$.

Potentiometric Titrations. All titrant solutions were prepared using distilled water that was further purified by passing through a Millipore Milli-Q reverse-osmosis cartridge system (resistivity 18 MΩ cm). The titrants were degassed by boiling for 1 h while being purged with argon. Solutions were stored under an atmosphere of purified argon (Ridox oxygen scavenger, Fisher) and Ascarite II (A. H. Thomas) scrubbers in order to prevent absorption of oxygen and carbon dioxide. Carbonate-free 0.1 M KOH was prepared from Baker Dilut-It concentrate and was standardized by titrating against potassium hydrogen phthalate using phenolphthalein as an indicator. Solutions of 0.1 M HCl were similarly prepared and were standardized by titrating against the KOH solution to the phenolphthalein end point. The combined pH glass electrode (Corning) filled with 3 M KCl (Corning filling solution) was calibrated in hydrogen ion concentration units ($p[H] = -\log [H^+]$) by titrating 2.000 mL of standardized HCl diluted in 50 mL of 0.100 M KCl (Mallinckrodt, ACS grade) with 4.200 mL of standardized KOH. Titrations were performed using a Dosimat 665 (Metrohm) piston buret and an Accumet 925 (Fisher) pH-meter or a Titrimo 702 SM buret with a built in pH-meter. All solutions were maintained at constant ionic strength (0.1 M KCl), under a nitrogen atmosphere and at constant temperature (25.0 ± 0.2 °C), by using a jacketed titration vessel fitted to a Neslab RTE-111 water bath. PC computers controlled both instruments.¹³ All values and errors (one standard deviation) reported represent the average of at least four independent experiments.

Spectrophotometric Titrations. The apparatus and methods for spectrophotometric titrations have been described in detail elsewhere.¹⁴

The path length of the quartz cell (Hellma, Suprasil) was either 1 or 10 cm. Once again, all solutions were maintained at constant ionic strength (0.1 M KCl), under a nitrogen atmosphere and at constant temperature (25.0 ± 0.2 °C), by using a jacketed titration vessel fitted to a Neslab RTE-111 water bath. To 40–50 mL of 0.1 M KCl were added ligand and metal from prepared solutions (2.0 mM and 0.1 M, respectively). After the $p[H]$ was decreased to about 2.0 with 1.0 M HCl, the ligands were titrated with standardized base to about $p[H]$ 7.0–8.0. The thermodynamic reversibility was checked by cycling titrations from low to high $p[H]$ and back to low $p[H]$. The data (absorbances at 151 wavelengths ranging between 250 and 400 nm, $p[H]$ values, and respective volumes of 20–60 spectra) were analyzed to determine the formation constants using the factor analysis program FINDCOMP and the nonlinear least-squares refinement program REFSPEC.¹⁵ All values and errors (one standard deviation) reported represent the average of at least four independent experiments.

Relaxivity Studies. ¹H NMR. The longitudinal water proton relaxation rate at 20 MHz was measured by using a Spinmaster spectrometer (Stelar, Mede, Italy) operating at 0.5 T; the standard inversion–recovery technique was employed (16 experiments, 4 scans). A typical 90°-pulse width was 3.5 ms, and the reproducibility of the T_1 data was $\pm 0.5\%$. The temperature was controlled with a Stelar VTC-91 air-flow heater equipped with a copper–constantan thermocouple (uncertainty of ± 0.1 °C). The proton $1/T_1$ NMRD profiles were measured on a Koenig-Brown field-cycling relaxometer over a continuum of magnetic field strengths from 0.000 24 to 1.2 T (corresponding to 0.01–50 MHz proton Larmor frequencies). The relaxometer operates under computer control with an absolute uncertainty in $1/T_1$ of $\pm 1\%$. Details of the instrument and of the data acquisition procedure are given elsewhere.¹⁶

¹⁷O NMR. Variable-temperature ¹⁷O NMR measurements were recorded on JEOL EX-90 (2.1 T) and EX-400 (9.4 T) spectrometers equipped with a 5 mm probe. A D₂O external lock and solutions containing 2.6% of the ¹⁷O isotope (Yeda) were used. The observed transverse relaxation rates were calculated from the signal width at half-height. Other details of the instrumentation, experimental methods, and data analysis have been previously reported.^{3,17}

Theory. The theory behind the water ¹H and ¹⁷O relaxation properties is presented in the Supporting Information and can be found in several references.^{3,18–20}

Results and Discussion

Synthesis. TREN-Me-3,2-HOPOSAM was synthesized as shown in Scheme 1. Reaction of 2-(benzyloxycarbonylsuccinyl)succin-

- (10) SAINT: SAX Area-Detector Integration Program, Version 4.024; Siemens Industrial Automation, Inc.: Madison, WI, 1994.
- (11) SHELXTL: Crystal Structure Analysis Determination Package; Siemens Industrial Automation, Inc.: Madison, WI, 1994.
- (12) SMART: Area-Detector Software Package; Siemens Industrial Automation, Inc.: Madison, WI, 1994.
- (13) Rodgers, S. J.; Lee, C. W.; Ng, C. Y.; Raymond, K. N. *Inorg. Chem.* **1987**, *26*, 1622.
- (14) Kappel, M.; Raymond, K. N. *Inorg. Chem.* **1982**, *21*, 3437.

- (15) Turowski, P. N.; Rodgers, S. J.; Scarrow, R. C.; Raymond, K. N. *Inorg. Chem.* **1988**, *27*, 474.
- (16) Koenig, S. H.; Brown, R. D., III. *NMR Spectroscopy of Cells and Organism*; CRC Press: Boca Raton, FL, 1987.
- (17) Aime, S.; Botta, M.; Fasano, M.; Paoletti, S.; Terreno, E. *Chem.—Eur. J.* **1997**, *3*, 1499.
- (18) Banci, L.; Bertini, I.; Luchinat, C. *Nuclear and Electron Relaxation*; VCH: Weinheim, Germany, 1991.
- (19) Freed, J. H. *J. Chem. Phys.* **1978**, *68*, 4034.
- (20) Powell, D. H.; Dhubhghaill, O. M. N.; Pubanz, D.; Helm, L.; Lebedev, Y. S.; Schlaepfer, W.; Merbach, A. E. *J. Am. Chem. Soc.* **1996**, *118*, 9333.

Scheme 2

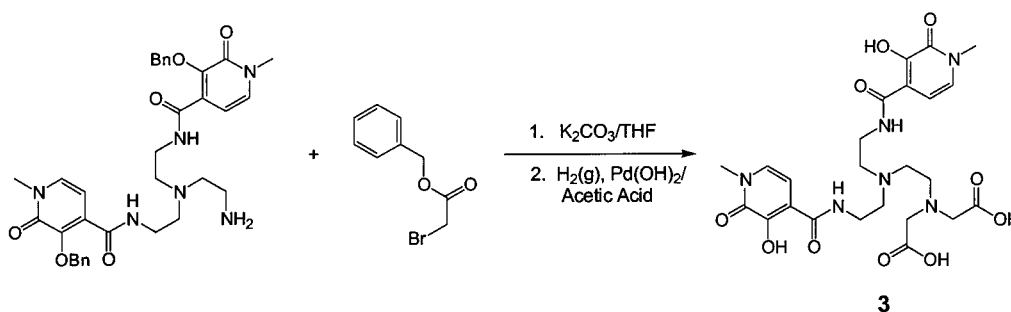


Table 1. Protonation and Formation Constants for Heteropodand Ligands and Gd^{3+} Complexes as Measured by Potentiometric or Spectrophotometric Titration ($I = 0.1$ (KCl); $T = 25$ °C)^a

	TREN-Me-3,2-HOPO ^{b,c}	TREN-Me-3,2-HOPOBAC ^d	TREN-Me-3,2-HOPOSAM ^b	TREN-Me-3,2-HOPOIAM ^b	TREN-Me-3,2-HOPOTAM ^b
log K_1	8.20(1)	9.53(4)	9.01(2)	8.35(2)	11.42(7)
log K_2	6.95(3)	7.30(2)	7.86(1)	7.20(2)	8.14(3)
log K_3	5.80(3)	6.53(1)	6.02(1)	5.99(1)	7.05(1)
log K_4	4.96(5)	3.23(3)	5.24(1)	5.05(5)	5.75(1)
log K_5	n/a	n/a	n/a	n/a	4.98(6)
log β_{110}	20.3(2)	14.8(2)	17.3(2)	16.5(1)	24.1(1)
log β_{111}	23.8(1)	22.2(3)	23.6(1)	21.2(2)	29.7(2)
log β_{112}	n/a	25.3(3)	27.9(1)	26.6(1)	34.3(2)
pGd	20.3	13.7	16.1	16.2	20.1

^a Numbers in parentheses correspond to the estimated standard deviations calculated from the variance/covariance matrix of at least four independent measurements. ^b Protonation constants measured by potentiometric titration; formation constants measured by spectrophotometric titration. ^c From ref 5. ^d Protonation and formation constants measured by potentiometric titration.

imide²¹ with the (Me-3,2-HOPO)₂TREN intermediate⁹ gave the benzyl-protected ligand (**1**). Deprotection with 1:1 glacial acetic acid/concentrated hydrochloric acid afforded the free ligand (**2**) as the hydrochloride salt.

The synthesis of TREN-Me-3,2-HOPOBAC is shown Scheme 2. The (Me-3,2-HOPO)₂TREN intermediate was mixed with an excess of benzyl 2-bromoacetate and anhydrous K_2CO_3 in dry THF. After the mixture was heated overnight at 60 °C, the protected ligand was isolated by flash silica column chromatography. Immediate deprotection by reductive hydrogenation (glacial acetic acid, 400 psi of $\text{H}_2(\text{g})$, 20% $\text{Pd}(\text{OH})_2/\text{C}$) afforded the free ligand as a white powder. The preparations of the other two ligands in this study were similar and are described in detail elsewhere.⁹ This methodology allows for the preparation of gram quantities of the desired ligands. In addition, the thiazolidine-activated intermediates in the synthesis of TREN-Me-3,2-HOPOIAM and TREN-Me-3,2-HOPOTAM react with a variety of amines for attachment of solubilizing, bioactive, or macromolecular components.⁹ Simple modifications of the salicylamide and bis(acetate) syntheses would also allow for facile derivatization.

Ligand Protonation Constants. The protonation constants for all of the heteropodands were determined by potentiometric titration.^{9,13} These values were required for further determination the stabilities of the heteropodand ligands with Gd^{3+} . The pK_a 's and standard deviations for ligands are listed Table 1. The titration results clearly demonstrate the influence of the mixed chelator design on the protonation behavior of the ligands relative to the parent compound. TREN-Me-3,2-HOPOSAM and TREN-Me-3,2-HOPOTAM are more basic than TREN-Me-3,2-HOPO.⁵ This is consistent with the basicity of the simple chelators, whose methylamide derivatives have pK_a 's of 8.03, 11.1/6.1, and 6.12 for the salicylamide, terephthalamide, and hydroxypyridinone chelators, respectively.^{22,23} TREN-Me-3,2-

HOPOTAM has protonation constants very similar to those of the parent compound, consistent with the similar protonation constants of the isophthalamide and HOPO chelators.²⁴ Finally, TREN-Me-3,2-HOPOBAC shows an intermediate behavior, with the first three pK_a 's being higher than those of the parent compound but with the last pK_a being much lower due to the strongly acidic acetate groups.

Stability Constants of the Ligands with Gd^{3+} . Of the heteropodand lanthanide complexes, only TREN-Me-3,2-HOPOBAC was sufficiently soluble to permit determination of the formation constants by potentiometry (Table 1). The overall formation constant (log β_{110}) of $\text{Gd}[\text{TREN-Me-3,2-HOPOBAC}]^-$ is 14.8(2), substantially lower than that of the parent complex (20.3).^{5,6} The conditional stability constant (pGd at 1 mM Gd^{3+} , 10 mM ligand, pH 7.4) of a metal–ligand complex is typically considered a better gauge of physiologically relevant complex stability than the overall stability constant.²⁵ The pGd value of 13.7 for $\text{Gd}[\text{TREN-Me-3,2-HOPOBAC}]^-$ is significantly lower than that of the parent complex (20.3)^{5,6} and slightly lower than that of $\text{Gd}[\text{DTPA-BMA}]$, which has the lowest conditional stability constant of all the commercially used MRI agents.

The stabilities of the heteropodand ligands TREN-Me-3,2-HOPOIAM, TREN-Me-3,2-HOPOTAM, and TREN-Me-3,2-HOPOSAM with Gd^{3+} were measured by spectrophotometric titration.¹⁵ The strong UV absorptions ($\pi \rightarrow \pi^*$) of the aromatic components of the ligands were monitored to follow the complexation reactions. Typical experimental conditions comprised 20–60 spectra, monitored between 200 and 400 nm, for a titration of each heteropodand in the presence of an equimolar

(21) Cohen, S. M.; Raymond, K. N. *Inorg. Chem.* **2000**, 39, 3624.

(22) Cohen, S. M.; Meyer, M.; Raymond, K. N. *J. Am. Chem. Soc.* **1998**, 120, 6277.

(23) Garrett, T. M.; Miller, P. W.; Raymond, K. N. *J. Am. Chem. Soc.* **1989**, 111, 128.

(24) Cohen, S. M. Ph.D. Dissertation, University of California, Berkeley, CA, 1998.

(25) Cacheris, W. P.; Quay, S. C.; Rocklage, S. M. *Magn. Reson. Imaging* **1990**, 8, 467.

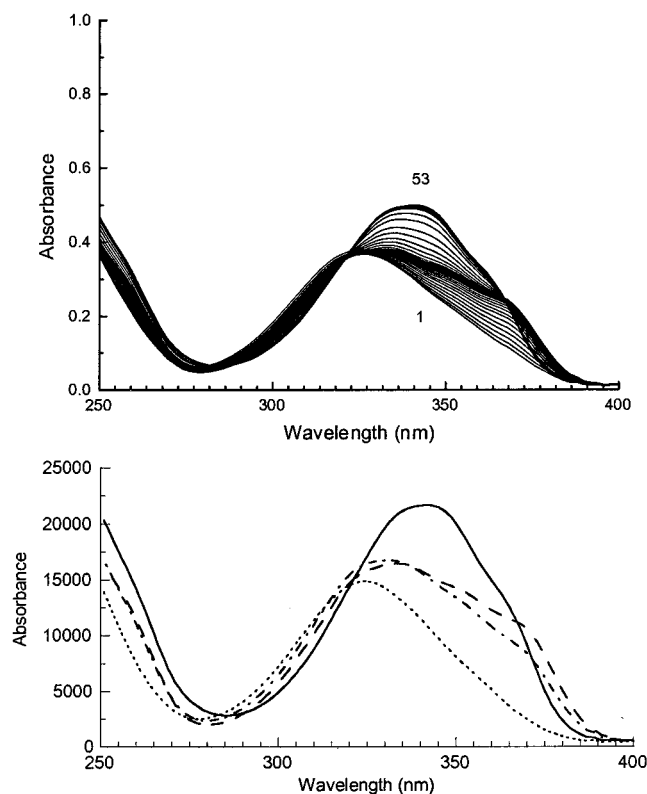


Figure 2. Representative data from spectrophotometric titration experiments: experimental (top) and calculated (bottom) spectra for a titration of TREN-Me-3,2-HOPOIAM with Gd³⁺. Factor analysis elucidated the presence of four species: LH₄ (dotted line), MLH₂²⁺ (dotted-dashed line), MLH⁺ (dashed line), and ML (solid line). *I* = 0.1 M (KCl); *T* = 25 °C.

amount of Gd³⁺. All three systems displayed substantial spectral changes upon metal complexation (see Figure 2 and Supporting Information). The absorbance maxima of the spectra generally shifted to lower energy as the pH was raised (pH ~4–5) with complicated multiple shoulder features at the longer wavelength ends of the transitions. Further increases in pH caused all of the spectral maxima to undergo substantial shifts to longer wavelengths. This large movement in the absorption wavelength maxima was coupled with a significant increase in the intensities of the bands. The final spectra corresponded to the fully formed Gd³⁺ complexes. At high pH (pH > 8), there was no change in the UV absorption spectra.

The speciations of TREN-Me-3,2-HOPOTAM, TREN-Me-3,2-HOPOIAM, and TREN-Me-3,2-HOPOSAM with Gd³⁺ are similar to that reported for the parent compound,⁵ with the observation of an extra species, the diprotonated complex GdLH₂.⁶ In fact, this species is also formed in the parent system, as has been revealed by recent investigations.^{6,26} The latter studies used a combination of spectral factor analysis,^{27,28} comparison of calculated and observed spectral band shapes, and superior potentiometric calibration procedures⁶ to more accurately examine the solution speciations. A close derivative of the parent compound with improved water solubility has been prepared, and thermodynamic analysis of its Gd³⁺ coordination chemistry has established the presence of an equivalent GdLH₂ species.⁶ The nonlinear least-squares refinement of the overall formation constant β_{110} included the ligand protonation constants obtained by potentiometric titration and the metal hydrolysis

equilibrium constants which were fixed to the literature values.²⁹ The calculated stability constants for the metal–ligand complexes are provided in Table 1. As judged from the pGd values, all of these ligands show satisfactory stability for consideration as MRI contrast agents. The two salicylate-derived compounds, TREN-Me-3,2-HOPOIAM and TREN-Me-3,2-HOPOSAM, have pGd values of 16.2 and 16.1, respectively. This is lower than the value of the parent compound^{5,6} but is competitive with those of commercially used MRI contrast agents. TREN-Me-3,2-HOPOTAM has a pGd value of 20.1, very similar to that of the parent compound.⁵ The stability of Gd[TREN-Me-3,2-HOPOTAM][−] is enhanced, in part, by the additional intramolecular hydrogen bond formed by the 2,3-dihydroxyterephthalamide unit.³⁰

Relaxometry. At 20 MHz, 25 °C, and pH 8.5 the relaxivities of the Gd³⁺ heteropodate complexes are 8.8, 7.2, 7.7, and 5.6 mM^{−1} s^{−1} for the terephthalamide, isophthalamide, salicylate, and bis(acetate) complexes, respectively. Although smaller than the parent compound,^{6,7} these complexes have relaxivities much higher than those of all currently available commercial contrast agents.^{2,3} The latter are monoaquo, enneacoordinated polyaminocarboxylate complexes with r_{1p}^H values in the range 3.5–4.8 mM^{−1} s^{−1}, under identical experimental conditions. At 20 MHz, the relaxivity of the aqueous solutions of small Gd³⁺ chelates under the rapid-exchange condition ($T_{1M}^H \gg \tau_M^H$, see eq 3, Supporting Information) receives comparable contributions from R_{1p}^{His} (~60%) and R_{1p}^{Hos} (~40%). The outersphere component has a slight dependence on the molecular size of a complex, through the parameters *a* and *D*, but its values are expected to be very similar for all of these systems (2.0–2.5 mM^{−1} s^{−1} at 25 °C).^{2–4} The inner-sphere term at 20 MHz is dominated by the τ_R/r_H^6 ratio (see eq 4, Supporting Information) and then increases with the molecular weight of the metal chelates. It follows that the large relaxivity enhancement observed for the heteropodand complexes reported here could be attributed to (a) a different hydration structure (parameter *q* in eq 3, Supporting Information), (b) a longer reorientational correlation time (τ_R) due to the increased molecular weight, or (c) a shorter distance (r_H) for the inner-sphere water molecule(s). More insight can be gained by plotting r_{1p}^H versus the molecular weight (Figure 3) for the heteropodate complexes, for the commercial MRI contrast agents Gd[DTPA]^{2−} (DTPA = 1,1,4,7,7-pentakis(carboxymethyl)-1,4,7-triazaheptane), Gd-[DTPA-BMA] (DTPA-BMA = 1,7-bis[(*N*-methylcarbamoyl)-methyl]-1,4,7-tris(carboxymethyl)-1,4,7-triazaheptane), Gd-[DOTA][−] (DOTA = 1,4,7,10-tetrakis(carboxymethyl)-1,4,7,10-tetraazacyclododecane), and Gd[HP-DO3A] (HP-DO3A = 10-(2-hydroxypropyl)-1,4,7-tris(carboxymethyl)-1,4,7,10-tetraazacyclododecane), and for Gd[DO3A] (DO3A = 1,4,7-tris(carboxymethyl)-1,4,7,10-tetraazacyclododecane), a macrocyclic complex with two inner-sphere water molecules (*q* = 2). The linear relationship observed confirms the dependence of r_{1p}^H on the tumbling rates of the complexes and the close similarity of the outer-sphere contributions and excludes significant variations in the distance values (r_H). Figure 3 also shows that the heteropodands can be divided into two groups with one (*q* = 1) and two (*q* = 2) inner-sphere water molecules. The relaxivity of Gd[DTPA-BMA] does not follow the expected behavior because of a limiting (long) τ_M value.^{31,32}

(26) O'Sullivan, B.; Raymond, K. N. Unpublished results.

(27) Tauler, R.; Smilde, A.; Kowalski, B. *J. Chemom.* **1995**, *9*, 31.

(28) Geladi, P.; Smilde, A. *J. Chemom.* **1995**, *9*, 1.

(29) Martell, A. E.; Motekaitis, R. M. *Determination and Use of Stability Constants*; VCH: New York, 1988.

(30) Hou, Z. Ph.D. Dissertation, University of California, Berkeley, CA, 1995.

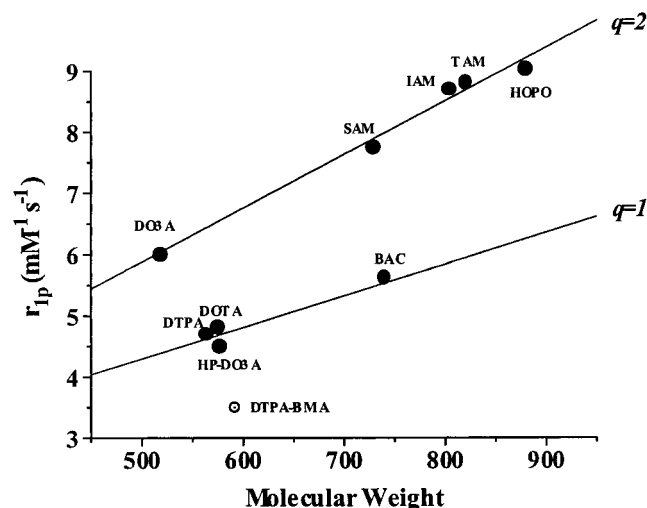


Figure 3. Plots of relaxivity (20 MHz, 25 °C) versus molecular weight for several Gd^{3+} MRI contrast agents. For these compounds, relaxivity increases linearly with molecular weight. The linear relationship gives a strong indication of the number of inner-sphere water molecules for these complexes.

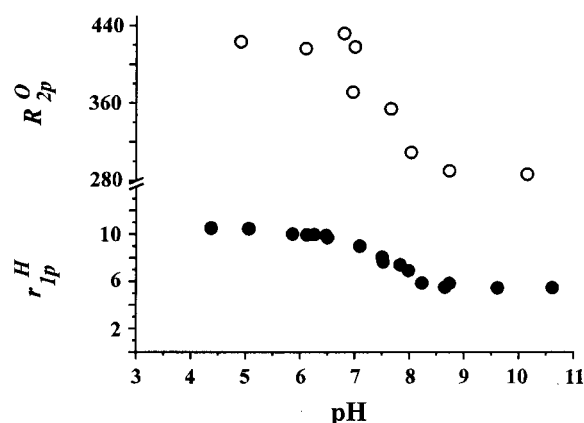


Figure 4. Plots of proton relaxivity ($\text{mM}^{-1} \text{s}^{-1}$; filled circles) at 25 °C and 20 MHz and of the ^{17}O transverse relaxation rate (s^{-1} ; open circles) at 25 °C and 12 MHz versus pH for $\text{Gd}[\text{TREN-Me-3,2-HOPOBAC}]^-$.

The ligand TREN-Me-3,2-HOPOBAC is expected to bind in a heptadentate fashion, using four HOPO oxygens, two acetate oxygens, and the acetate tertiary nitrogen. The presence of a single metal-bound water molecule in $\text{Gd}[\text{TREN-Me-3,2-HOPOBAC}]^-$ suggests that this heptadentate ligand forms an overall 8-coordinate lanthanide complex like the parent compound.⁵ The relaxivity of $\text{Gd}[\text{TREN-Me-3,2-HOPOBAC}]^-$ is strongly dependent upon solution pH (Figure 4). The relaxivity is constant between pH 8 to 11, markedly increases upon lowering the pH, and below pH 6 reaches a plateau of about $10.4 \text{ mM}^{-1} \text{s}^{-1}$. The increase in relaxivity corresponds to an increase of one water molecule ($q = 2$) in the Gd^{3+} inner coordination sphere. This is clearly confirmed by the fact that the profile of the ^{17}O transverse relaxation rate vs pH, which only reports the effects associated with the metal-bound water molecules, reproduces quite closely the ^1H relaxivity behavior for $\text{Gd}[\text{TREN-Me-3,2-HOPOBAC}]^-$, also shown in Figure 4. The observed relaxivity behavior can be explained in terms of the speciation of the lanthanide complex as a function of pH.

On the basis of the constants determined by potentiometric titration (Table 1), the complex undergoes a transition between pH 6 and 8, with the dominant species at pH 8 being the unprotonated (ML^-) complex, but by pH 6, the monoprotonated complex (MLH) is the sole (>90%) component (see the Supporting Information). The protonation likely occurs at the acetate bridgehead nitrogen, breaking coordination to the metal ion. This reduces the denticity of the ligand from hepta- to hexadentate and provides an additional site for water coordination, subsequently increasing relaxivity. The pH-dependent relaxivity is the result of a structural reorganization of the ligand around the metal center caused by a change in the protonation state of the complex.

The ligands TREN-Me-3,2-HOPOSAM, TREN-Me-3,2-HO-POTAM, and TREN-Me-3,2-HOPOIAM were expected to bind in a hexadentate fashion to the lanthanide ion, allowing for coordination of at least two inner-sphere water molecules. The relaxivity data (vide infra) support this hypothesis, suggesting that the lanthanide complexes are 8-coordinate (like the parent complex)⁵ with two inner-sphere water molecules ($q = 2$). Analogous to $\text{Gd}[\text{TREN-Me-3,2-HOPOBAC}]^-$, these complexes also show pH-dependent relaxivity profiles. The relaxivity increases with a lowering of pH from 5 to 3 for $\text{Gd}[\text{TREN-Me-3,2-HOPOBAC}]^-$, from 6 to 3 for $\text{Gd}[\text{TREN-Me-3,2-HOPOIAM}]^-$, and from 7 to 4 for $\text{Gd}[\text{TREN-Me-3,2-HOPOSAM}]^-$. This behavior reflects the increase of the hydration number from $q = 2$ to $q = 3$ upon protonation of the ligand and subsequent rearrangement of the coordination polyhedra (see the Supporting Information). Ligand protonation likely occurs at the 2-hydroxyisophthalamide, 2,3-dihydroxyterephthalamide, and salicylamide chelators for $\text{Gd}[\text{TREN-Me-3,2-HOPOIAM}]^-$, $\text{Gd}[\text{TREN-Me-3,2-HOPOTAM}]^-$, and $\text{Gd}[\text{TREN-Me-3,2-HOPOSAM}]^-$, respectively (unpublished data).²⁴ Prototropic exchange may also contribute to the increase in relaxivity at lower pH values.

NMRD Profiles. Nuclear magnetic resonance dispersion (NMRD) profiles can be used to determine the values of the parameters that contribute to the relaxivity of a Gd^{3+} complex.^{2,3} The experiment involves measuring the magnetic field strength (Larmor frequency) dependence of the solvent proton longitudinal relaxation rate in the presence of a Gd^{3+} complex. This field dependence is measured at several temperatures to improve the fitting of several parameters. Figure 5 shows the NMRD profiles and calculated fittings for the complexes at 15, 25, and 39 °C.

Numerous papers are available on the details of the fitting of NMR dispersion profile data.^{2,3} For the purposes of this work, the experimental data and parameters obtained from these data will be presented and discussed in the context of (1) how HOPO-based complexes compare with commercial MRI contrast agents, (2) how the heteropodate structures compare with the parent complex (and a more soluble analogue of the parent complex, $\text{Gd}[\text{SerTREN-Me-3,2-HOPOTREN}]$),^{7,8} and (3) the overall efficacy of these complexes as MRI contrast media.

As shown in Figure 5, the NMRD profiles of the HOPO-based ligands first drop (in the range from 1 to 10 MHz) and then rise with increasing magnetic field strength (increasing Larmor frequency). These profiles are distinct from the NMRD profiles of commercial polyaminocarboxylate complexes, which begin to drop off at ~ 1 MHz and continue to drop with increasing field strength. This difference is important because clinical MRI experiments are performed at frequencies between 20 and 60 MHz,²⁻⁴ a region where polyaminocarboxylate complexes reach a minimum in relaxivity and HOPO-based

(31) Gonzalez, G.; Pagliarin, R.; Sisti, M.; Terreno, E. *J. Phys. Chem.* **1994**, 98, 53.

(32) Aime, S.; Botta, M.; Fasano, M.; Paoletti, S.; Anelli, P. L.; Uggeri, F.; Virtuani, M. *Inorg. Chem.* **1994**, 33, 4707.

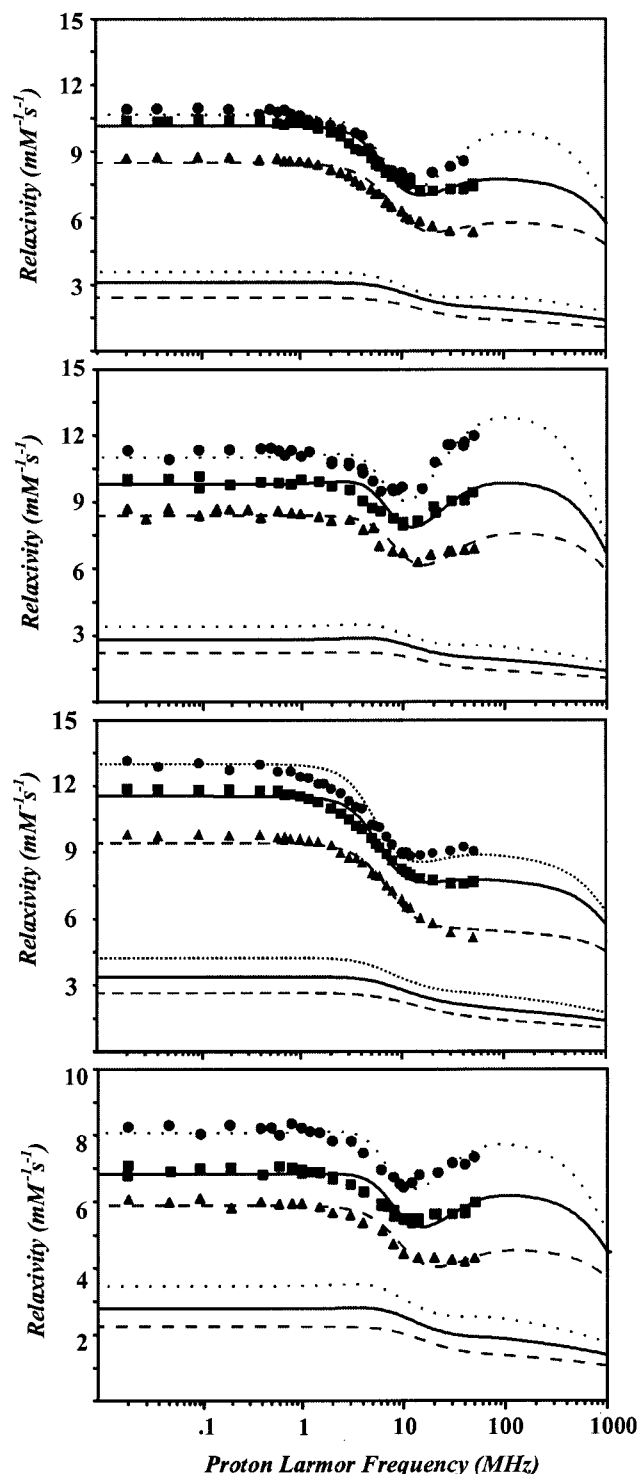


Figure 5. Nuclear magnetic relaxation dispersion (NMRD) profiles for the Gd³⁺ heteropodate complexes at 15 (circles), 25 (squares), and 39 °C (triangles). From top to bottom: Gd[TREN-Me-3,2-HOPOIAM] (pH 9.0), Gd[TREN-Me-3,2-HOPOTAM]⁻ (pH 7.6), Gd[TREN-Me-3,2-HOPOSAM] (pH 9.0), and Gd[TREN-Me-3,2-HOPOBAC]⁻ (pH 9.2).

complexes increase in relaxivity. The shape of these profiles is due to the higher molecular weight of the HOPO-based chelates and the subsequent increase in the rotational correlation time (τ_R) that allows the field dependence of the electronic relaxation time to become visible (see eqs 5–7, Supporting Information). On a much larger scale, similar NMRD profiles have been shown for polyaminocarboxylate ligands that are noncovalently bound to human serum albumin (HSA).^{3,33}

Table 2 lists the parameters obtained from fitting the NMRD profiles for all four Gd³⁺ complexes. The parameters are (1) the zero-field value of the electronic relaxation time (τ_{SO} , which is the value of τ_{1s} at zero magnetic field strength), (2) the correlation time of the fluctuation of the transient zero-field splitting (τ_V), (3) the rotational correlation time (τ_R), and (4) the distance between the water protons and the metal-centered unpaired electron spin (r_H).³

The metal-proton distances of the coordinated water molecules (r_H) for the HOPO-based complexes are slightly smaller than those found in commercial contrast agents.^{2–4} The shorter distances between the paramagnetic centers and the water protons do make small contributions to the higher relaxivities of the HOPO-based compounds. Furthermore, r_H is strongly correlated with the rotational correlation time (τ_R) and thus its variation may be insignificant. More importantly, all of the HOPO-based systems have very long rotational correlation times (τ_R) relative to those of the polyaminocarboxylate complexes. This contributes significantly to their high relaxivities, as shown previously in Figure 3, where the increasing molecular weights of the complexes correspond to a linear increase with relaxivity. Finally, the NMRD fittings indicate that Gd[TREN-Me-3,2-HOPOIAM], Gd[TREN-Me-3,2-HOPOTAM]⁻, and Gd[TREN-Me-3,2-HOPOSAM] have q values of 2, whereas Gd[TREN-Me-3,2-HOPOBAC]⁻ has a q value of 1. In the cases of Gd[TREN-Me-3,2-HOPOIAM], Gd[TREN-Me-3,2-HOPOTAM]⁻, and Gd[TREN-Me-3,2-HOPOSAM], the doubling of the q values nearly doubles the values of the relaxivities of the former compounds over those of the polyaminocarboxylate complexes.

¹⁷O NMR VT Relaxivity Behavior. The residence water lifetime τ_M is a measure of how long a water molecule remains bound to the lanthanide center before dissociating into the bulk solvent. This value can be determined by measuring the transverse ¹⁷O NMR relaxation time at various temperatures. Typically, the residence lifetime is not a limiting parameter for the relaxivity of a complex at physiological temperature.^{31,32} However, recent studies have shown that, for macromolecular systems with extremely long rotational correlation times, the water exchange rate can become the primary limiting factor for attaining high relaxivity.^{1,34} In these macromolecular systems, long rotational correlation times were obtained with noncovalent HSA–DOTA adducts and dendrimer–DOTA conjugates. However, the water molecules bound to the lanthanide complexes did not dissociate quickly enough (large τ_M), diminishing the effect of the long τ_R in relaxing the bulk solution.

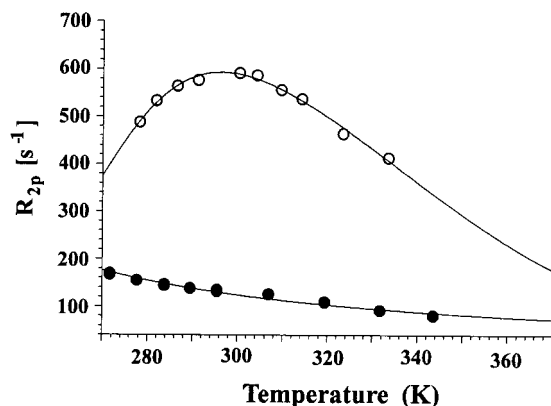
A primary goal of the heteropodand design was attachment to macromolecular structures and therefore prompted the determination the water exchange rates for these compounds. If the water exchange rates of the heteropodand derivatives were not sufficiently rapid, then any macromolecular derivatives would suffer from the same limitations as the previously studied DOTA- and DTPA-based macromolecular systems.^{33–37} Variable-temperature ¹⁷O NMR experiments require higher concen-

- (33) Aime, S.; Botta, M.; Fasano, M.; Geninatti Crich, S.; Terreno, E. *Coord. Chem. Rev.* **1999**, *321*, 185.
- (34) Toth, E.; Pubanz, D.; Vauthey, S.; Helm, L.; Merbach, A. E. *Chem.—Eur. J.* **1996**, *12*, 1607.
- (35) Aime, S.; Botta, M.; Fasano, M.; Crich, S. G.; Terreno, E. *J. Bioinorg. Chem.* **1996**, *1*, 312.
- (36) Aime, S.; Botta, M.; Geninatti Crich, S.; Giovenzana, G. B.; Pagliarin, R.; Piccinini, M.; Sisti, M.; Terreno, E. *J. Bioinorg. Chem.* **1997**, *2*, 470.
- (37) Wiener, E. C.; Brechbiel, M. W.; Brothers, H.; Magin, R. L.; Gansow, O. A.; Tomalia, D. A.; Lauterbur, P. C. *Magn. Reson. Med.* **1994**, *31*, 1.

Table 2. Parameters Obtained from Nuclear Magnetic Resonance Dispersion (NMRD) Profile Fittings

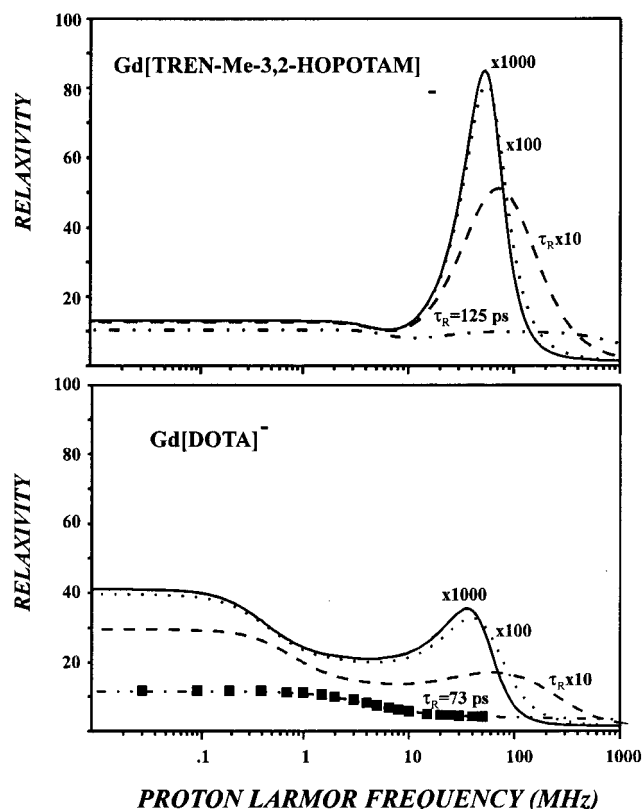
	Gd[TREN-Me-3,2-HOPOBAC] [−]			Gd[TREN-Me-3,2-HOPOSAM]			Gd[TREN-Me-3,2-HOPOTAM] [−]			Gd[TREN-Me-3,2-HOPOIAM]		
<i>T</i> (°C)	15	25	39	15	25	39	15	25	39	15	25	39
τ_{SO} (ps) ^a	43	39	39	72	67	65	42	41	38	47	52	49
τ_{V} (ps)	18	15	11	21	20	16	20	18	13	14	16	11
τ_{R} (ps)	131	110	77	103	94	66	160	125	96	123	99	74
<i>q</i>	1	1	1	2	2	2	2	2	2	2	2	2
<i>r</i> _H (Å)	2.95	2.95	2.95	3.10	3.10	3.10	3.05	3.05	3.05	3.10	3.10	3.10

^a τ_{SO} is related to Δ^2 and τ_{V} by the relation $\tau_{\text{SO}} = (12\Delta^2\tau_{\text{V}})^{-1}$.

**Figure 6.** Plots of the ¹⁷O transverse relaxation rate versus temperature for Gd[TREN-Me-3,2-HOPOTAM][−] (21.6 mM, pH 8.5, 9.4 T; filled circles) and Gd[DO3A] (50 mM, pH 7.5, 2.1 T; open circles).

trations than NMRD measurements. Only the most soluble complexes Gd[TREN-Me-3,2-HOPOTAM][−] and Gd[TREN-Me-3,2-HOPOBAC][−] could be evaluated by ¹⁷O NMR methods at 9.4 and 2.1 T, respectively (Figure 6). For comparison, the data for Gd[DO3A] (at 2.1 T) are presented, which demonstrate a typical profile for an intermediate-exchange system with a τ_{M} of about 160 ns at 25 °C.³⁸ The profile for Gd[TREN-Me-3,2-HOPOTAM][−] (and Gd[TREN-Me-3,2-HOPOBAC][−]; data not shown) is notably distinct from that of Gd[DO3A] and is indicative of an extremely rapid water exchange process characterized by a τ_{M} (at 25 °C) of about 10–15 ns (see the Supporting Information). The values of the exchange rates cannot be determined with high accuracy by the experiment because the ¹⁷O relaxation is not limited by the short τ_{M} but rather by the longitudinal electron spin relaxation time (τ_{1s}). The water exchange rates are only 1 order of magnitude slower than that of the aqua ion and 1–2 orders of magnitude faster than those found for commercial MRI contrast agents.^{2–5} These rapid exchange rates are also nearly optimal for a slowly rotating MRI contrast agent.³⁴ The data suggest that macromolecular-based derivatives of the heteropodand ligands will not be limited by water exchange, as was found for DTPA- and DOTA-based systems. This is further illustrated by the simulated NMRD profiles of Gd[TREN-Me-3,2-HOPOTAM][−] and Gd[DOTA][−] as functions of increasing τ_{R} (Figure 7).^{34,37}

Although the lanthanide complexes of TREN-Me-3,2-HOPOIAM and TREN-Me-3,2-HOPOSAM were too insoluble to directly study by ¹⁷O NMR experiments, their exchange rates could be estimated by an indirect method. The temperature dependence of the ¹H relaxivity of a complex can yield useful qualitative information about the water exchange rate when the solubilities of the samples preclude analysis of the ¹⁷O NMR data.³⁸ Different exchange regimes are possible (see eq 3, Supporting Information): (1) rapid exchange ($\tau_{\text{M}} \ll T_{1\text{M}}^{\text{H}}$),

**Figure 7.** Simulated ¹H relaxivity profiles (mM^{−1} s^{−1}) at 25 °C for Gd[TREN-Me-3,2-HOPOTAM][−] (top) and Gd[DOTA][−] (bottom) with varying reorientational correlation times τ_{R} . The lower curve in each case represents the fitted experimental NMRD profile.

where the relaxivity increases with decreasing temperature (τ_{R} becomes longer and $T_{1\text{M}}^{\text{H}}$ decreases); (2) slow exchange ($\tau_{\text{M}} \gg T_{1\text{M}}^{\text{H}}$), where the relaxivity depends on $1/\tau_{\text{M}}$ and therefore decreases with decreasing temperature; and (3) intermediate exchange (τ_{M} and $T_{1\text{M}}^{\text{H}}$ have the same order of magnitude), where there is little dependence of the relaxivity on temperature. The temperature-dependent relaxivity profiles for Gd[TREN-Me-3,2-HOPOIAM] and Gd[TREN-Me-3,2-HOPOSAM] increase exponentially with decreasing temperature (see the Supporting Information), indicating that they lie in the rapid-exchange regime (are not dependent on τ_{M}) and that the water exchange lifetimes are well below 100 ns.

As first suggested when the Gd[TREN-Me-3,2-HOPO] complex was reported,⁵ the reason for the rapid water exchange rate seems likely to be a low-energy barrier between a 9-coordinate tris(aqua) complex intermediate and the observed 8-coordinate bis(aqua) complex, both of which have similar stabilities. This is the same reason that water exchange for the lanthanide aqua ions is so rapid. The early-lanthanide aqua complexes are 9-coordinate, and the smaller late-lanthanide aqua ions are 8-coordinate. In both cases, the intermediate (dissociative for coordination number 9 and associative for coordination

(38) Aime, S.; Botta, M.; Crich, S. G.; Giovenzana, G.; Pagliarini, R.; Sisti, M.; Terreno, E. *Magn. Reson. Chem.* **1998**, *36*, S200.

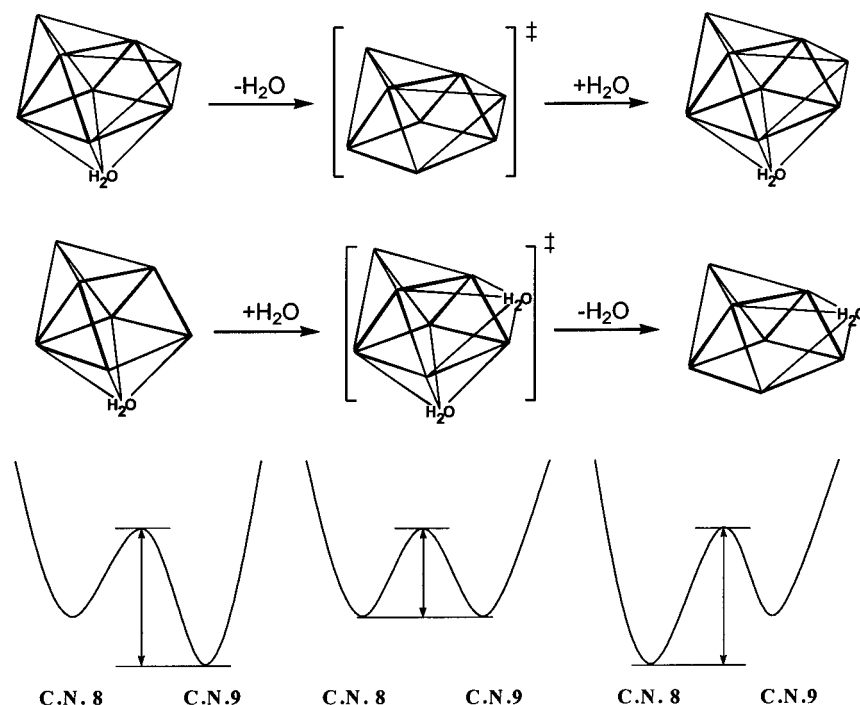


Figure 8. Water exchange pathways for Gd³⁺ complexes (aminocarboxylate and hydroxypyridinonate) that interconvert between 8- and 9-coordinate (upper panel). Free energy diagrams for water exchange: (left) 9-coordinate ground state; (right) 8-coordinate ground state; (middle) CN 8 and 9 equal in energy (lower panel).

number 8) is readily accessible (Figure 8). The commercial contrast agents have 9-coordinate ground state geometries with no 8-coordinate geometries observed, even for the smaller late lanthanides. Hence, the complexes exchange water through dissociative processes that go to relatively unstable 8-coordinate intermediates. In a series where the larger metal ions are 9-coordinate and the smaller ones are 8-coordinate, there will be an ionic radius where 9- and 8-coordinate complexes are equal in energy. At that point, the associative (8- to 9-coordinate) and dissociative (9- to 8-coordinate) exchange rates are identical and the rate of exchange is maximum.

Our expectation that the energy difference between the 8-coordinate and 9-coordinate structures for the HOPO complexes is very low is here confirmed. As previously described,⁵ the structure of Gd[TREN-Me-3,2-HOPO] is an 8-coordinate square antiprism with six HOPO oxygen donors and two water molecules. However, the crystal structure of same ligand complexed with an early-lanthanide ion, namely, La[TREN-Me-3,2-HOPO], has both an 8- and a 9-coordinate lanthanide metal center in the unit cell (Figure 9). The coordination geometry of one metal center (La(2)) is a square antiprism comprising the six HOPO oxygens, one disordered solvent (mixed DMSO and methanol), and an amide oxygen from the neighboring La(1)[TREN-Me-3,2-HOPO] molecule. The other metal center (La(1)) is a monocapped square antiprism composed of the six HOPO oxygens, one methanol molecule, and two amide oxygens from the neighboring La(2)[TREN-Me-3,2-HOPO] molecule (Table 3).^{10–12} The presence of both coordination numbers in the same crystal lattice indicates that the coordination environments of these two metal ions (La(1) and La(2)) must be very similar in energy. The structure demonstrates that the ligand can easily accommodate both coordination numbers for the lanthanide ions. The La³⁺ and Gd³⁺ structures taken together show that the TREN-Me-3,2-HOPO ligand allows free interchange between 8- and 9-coordinate complexes. The stability of both coordination numbers is consistent with the rapid rate of water exchange for the HOPO-based complexes:

the ligand provides a low barrier for interconversion between the two states, resulting in rapid solvent exchange (*vide infra*). Further confirmation of this proposed mechanism can be obtained by the use of variable-pressure NMR experiments, which are capable of distinguishing between an associative and a dissociative exchange mechanism by measuring the volume of activation.³⁹

Conclusions

The syntheses, solution thermodynamics, and relaxivity results for four novel HOPO-based heteropodand ligands have been presented. Potentiometric and spectrophotometric titrations have shown that at least three of the four complexes possess satisfactory thermodynamic stabilities to be considered as MRI contrast agents. All of the compounds show high relaxivities relative to those of commercially available contrast agents, although the heteropodate complexes have somewhat lower relaxivities than those found for tris(hydroxypyridinonate) complexes.^{5,7} The high relaxivities of these compounds can be attributed, in part, to several common features, including long rotational correlation times and short metal–water bond distances. The complexes also have rapid water exchange rates, as determined by ¹⁷O NMR and variable-temperature relaxivity measurements. The rapid exchange rates can be explained in terms of a low-energy barrier between the 8- and 9-coordinate complexes, as evidenced by the structure of La[TREN-Me-3,2-HOPO]. These rapid exchange rates also make the heteropodate complexes attractive candidates for preparing macromolecular MRI contrast agents.

Despite these common features, the compounds can be divided into two classes on the basis of the number of coordinated inner-sphere water molecules. A *q* value of 2 was inferred for Gd[TREN-Me-3,2-HOPOIAM], Gd[TREN-Me-3,2-

(39) Frey, U.; Merbach, A. E.; Powell, D. H. In *Solvent Exchange on Metal Ions: A Variable NMR Approach*; Delpuech, J.-J., Ed.; John Wiley & Sons: Chichester, U.K., 1995; p 263.

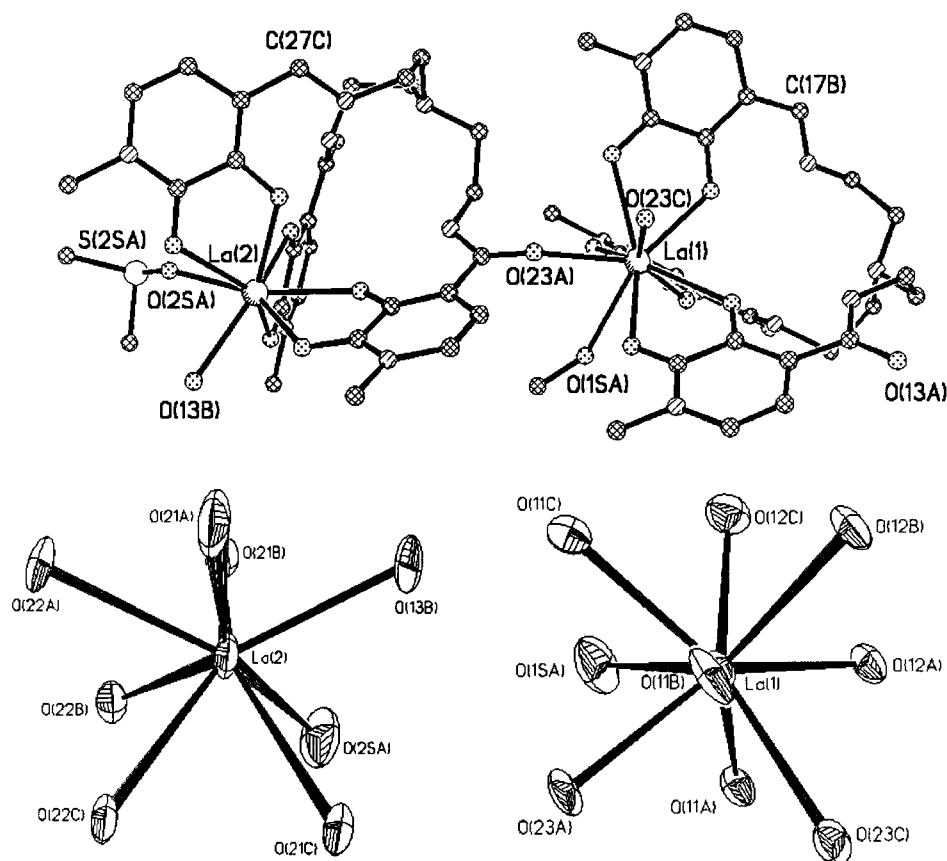


Figure 9. Structural diagrams (ORTEP) of La[TREN-Me-3,2-HOPO]. The asymmetric unit (top) contains two complexes of La[TREN-Me-3,2-HOPO] connected by amide oxygen coordination. The La(1) complex (bottom right, 9-coordinate monocapped square antiprism) is viewed down the C_4 axis, and the La(2) complex (bottom left, 8-coordinate square antiprism) is viewed perpendicular to the C_4 axis. The structure suggests that the 8- and 9-coordinate geometries are very similar in energy, allowing for rapid solvent exchange.

Table 3. Crystal Data and Structure Refinement Details for La[TREN-Me-3,2-HOPO]

fw	844.24
temp	146(2) K
crystal system	triclinic
space group	$P1$
unit cell dimensions	$a = 15.6963(2) \text{ \AA}$ $\alpha = 61.981(1)^\circ$ $b = 16.9978(1) \text{ \AA}$ $\beta = 75.680(1)^\circ$ $c = 17.1578(2) \text{ \AA}$ $\gamma = 71.600(1)^\circ$
V, Z	$3807.69(7) \text{ \AA}^3, 4$
density (calcd)	1.473 g cm^{-3}
crystal size	$0.20 \times 0.10 \times 0.06 \text{ mm}$
no. of reflns collected	20 526
no. of indep reflns	12 855 [$R(\text{int}) = 0.020$]
no. of data/restraints/params	8738/52/917
goodness-of-fit on F^2 ^a	1.038
final R indices [$I > 2\sigma(I)$] ^b	$R1 = 0.0710, wR2 = 0.1659$
R indices (all data) ^b	$R1 = 0.1131, wR2 = 0.1880$
largest diff peak and hole	$+2.034$ and $-1.873 \text{ e \AA}^{-3}$

^a $\text{GOF} = [\sum w(|F_o| - |F_c|)^2 / (N_o - N_v)]^{1/2}$, where $w = 1/(\sigma^2|F_o|)$. ^b $R1 = \sum ||F_o| - |F_c|| / \sum |F_o|$; $wR2 = [\sum w(F_o^2 - F_c^2)^2 / \sum wF_o^4]^{1/2}$.

HOPOTAM][−], and Gd[TREN-Me-3,2-HOPOSAM], which contributes to the particularly high relaxivities of these complexes. However, Gd[TREN-Me-3,2-HOPOBAC][−] has only one inner-sphere water molecule. In addition, all of the complexes display pH-dependent relaxivity profiles. The pH dependence can be correlated to the solution thermodynamics, which indicate that the metal complexes become protonated near or below neutral pH. Protonation of the metal complexes causes structural

changes that make the metal centers more accessible to water molecules and increases relaxation of the bulk solvents.

The mixed ligand design strategy is a facile and straightforward means to access novel ligand structures with several tunable properties. This method has produced several promising leads for the development of new MRI contrast agents. Starting with HOPO-based systems, we prepared complexes that possess high thermodynamic stabilities, high relaxivities, and rapid water exchange rates. Continued investigations into heteropodand “mixed” ligand systems, with other novel binding groups substituting for the third HOPO chelator, should contribute to the further development of new MRI contrast agents.

Acknowledgment. S.M.C. thanks Dr. Brendon O’Sullivan for help with the solution thermodynamics analysis. This work was supported in part by NIH Grant AI11744 and by the Director, Office of Energy Research, Office of Basic Energy Sciences, Chemical Sciences Division, U.S. Department of Energy, under Contract No. DE-AC03-76F00098. S.A. and M.B. acknowledge the MURST and CNR (Legge 95/95) for financial support.

Supporting Information Available: Plots of potentiometric titration data, spectrophotometric titration data, species distributions of metal complexes, and relaxivity versus pH/temperature data, a listing of parameters obtained from ¹⁷O relaxation data as a function of temperature, and text plus equations presenting the theory behind relaxation measurements. This material is available free of charge via the Internet at <http://pubs.acs.org>.

IC000563B